



# INTERNATIONAL CENTRE FOR THEORETICAL PHYSICS

CORE LEVEL SHIFTS IN GROUP IV  
SEMICONDUCTORS AND SEMIMETALS

Soe Yin

and

E. Tosatti



**INTERNATIONAL  
ATOMIC ENERGY  
AGENCY**



**UNITED NATIONS  
EDUCATIONAL,  
SCIENTIFIC  
AND CULTURAL  
ORGANIZATION**

**1981 MIRAMARE-TRIESTE**



International Atomic Energy Agency  
and  
United Nations Educational Scientific and Cultural Organization  
INTERNATIONAL CENTRE FOR THEORETICAL PHYSICS

CORE LEVEL SHIFTS IN GROUP IV SEMICONDUCTORS  
AND SEMIMETALS

Soe Yin\* and E. Tosatti

International Centre for Theoretical Physics, Trieste, Italy  
and  
International School for Advanced Studies (SISSA), Trieste, Italy

ABSTRACT

We calculate the core level binding energy shift from the isolated atom to the crystalline solid, for group IV elemental semiconductors. This is done by simple extension of Johansson and Martensson's scheme for metals. We show that the core level energy in a nonmetal must be measured by the photo absorption ("core exciton") threshold rather than by photo emission. As a byproduct, a simple scheme is also devised to evaluate impurity heats of solutions in semiconductors.

MIRAMARE - TRIESTE  
August 1981

\* Permanent Address: Physics Department, Arts & Science University,  
Rangoon, Burma.

.1 INTRODUCTION

During the last two decades a considerable amount of experimental work has been devoted to the investigation of core-level binding energies. The number of core levels and their binding energies are characteristic for a given element. The energy of an electron in a tightly bound state is determined by the attractive potential of the nuclei and the repulsive core coulomb interaction with all the other electrons. A change in the chemical environment of a particular atom involves a spatial rearrangement of the valence charges of this particular atom and different potential created by the nuclear and electronic charges on all the other atoms in the solid. It has now been well established that the exact value of the core-level binding energy measured for a given element depends on the chemical environment of that element. (1-3)

The core level binding energies of free atoms become systematically lowered by several eV when they are condensed to form a crystalline solid. A calculation of the energy shift for atom to solid will be the object of this work. The core-level binding energy shifts are given by the difference of two binding energies (4)

$$\begin{aligned} E_c &= ( E^A(n_c-1) - E^A(n_c) ) - ( E^S(n_c-1) - E^S(n_c) ) \\ &= E_c^A - E_c^S \end{aligned} \quad (1)$$

where  $E(n_c)$  is the total binding energy of the system considered as a function of the number of electrons  $n_c$  in a particular core level. The subscript A and S indicate the binding energies for the free atom and solid respectively. Here both binding energies are referred to the vacuum level.

One can, in general, decompose this shift into three contributions which are due to configuration changes, chemical shifts and relaxation shifts<sup>(4)</sup>. The configuration shift is the change in the core-level binding energy due to changing the configuration (the distribution of electrons among s, p, and d states) of the free atom into a configuration similar to that which the atom will adopt in the solid. The chemical shift is the displacement of the core level by changes in the chemical environment before an electron is removed from the level. The relaxation effect is associated with drastic arrangement of the electrons due to the removal of the electron from the core level. This rearrangement involves a flow of negative charge towards the hole created in the photoemission process in order to screen the suddenly appearing positive charge. The screening lowers the energy of the hole state left behind and therefore lowers the binding energy as well. Only in a few cases these contributions to the total shift have been evaluated by making use of some theoretical models for the metals, ionic solids and some intermetallic compounds<sup>(5,6)</sup>. This is however in general a very difficult task.

Recently a simple alternative theoretical scheme has been proposed by Johansson and Martensson (JM)<sup>(7)</sup> which has many practical merits. In this scheme one obtains a direct and simple relationship between the binding of a core level for the free atom  $E_c^A$

and the same core level in the metallic state of the atom relative to the fermi level  $E_{c,F}^S$  in terms of other experimental quantities such as the atomic ionization energies and the impurity heat of mixing. This scheme, based on a Born-type cycle, works very nicely and effectively for most of the metallic solids and the results are in good agreement with all known experimental results. However, JM have applied it only to metallic elements due to difficulties both of principle and of practical nature in applying it to semiconductors and insulators.

In the present work we extend JM's scheme to make it applicable also as well to the group IV semiconductors and semimetals. This is done by making two modifications to JM's scheme. The first one is connected with the measurement of  $E_c^S$ . In a nonmetal the core-binding energy must be obtained by the core  $\rightarrow$  conduction photoabsorption threshold, the so called "core-exciton"<sup>(8)</sup>, rather than the photoemission threshold. This final state insures complete screening around the core hole by the ejected electron, which is brought into the bound core-exciton level. Complete screening is necessary if one is to identify - as is done in JM's scheme - the core-excited atom with a neutral (Z+1) impurity. The second modification is associated with the evaluation of the impurity heat of solution for the semiconductors. Miedema's<sup>(9)</sup> empirical scheme cannot be used in this case. One can evaluate this quantity for the semiconductor by using e.g Van Vechten's<sup>(10)</sup> semi-empirical scheme. Alternatively one can use a tetrahedral  $sp^3$ -hybrid tight-binding cluster model. We consider both methods in the present work.

With above modifications JM's scheme becomes effectively applicable to the group IV semiconductors and semimetals as well and thus we are able to calculate the core-level binding energy shifts for these elements. We find that the agreement with the available experimental results are generally in the order of 1eV , which is rather satisfactory, in view of the simplicity of the scheme.

## 2.1. METALLIC SOLIDS (JM'S SCHEME)

For metallic solids, the core ionization process can be described by a simple picture with the following two basic assumptions,

- the core ionization is to be considered as taking place at a particular atomic site in the solid, and
- the site from which the core electron is ejected will have to become totally screened by the surrounding electrons.

This implies that the initial state before core ionization is the perfect metal and the final state after core ionization is a core-hole impurity site which is completely screened in an otherwise perfect crystal. The "equivalent cores approximation" or (Z+1) approximation<sup>(11)</sup> can then be applied to the final state. With this approximation , a core-hole site is (quite accurately) replaced by a (Z+1) atom and the final state resulting from the photo-ejection of the core electron can be described as a (Z+1) atomic impurity in the original Z metal.

This final state can also be reached from the original perfect metallic state by a Born-Haber cycle. This is illustrated in Fig.(1) after JM. The procedure involved in this cycle is as follows. First, a Z atom is extracted from the solid at the cost of the cohesive energy  $E_{coh}^Z$ . This atom is subsequently core-ionized, this costs the free atom core-binding energy  $E_c^A$ . The (z+1)-approximation is applied to this

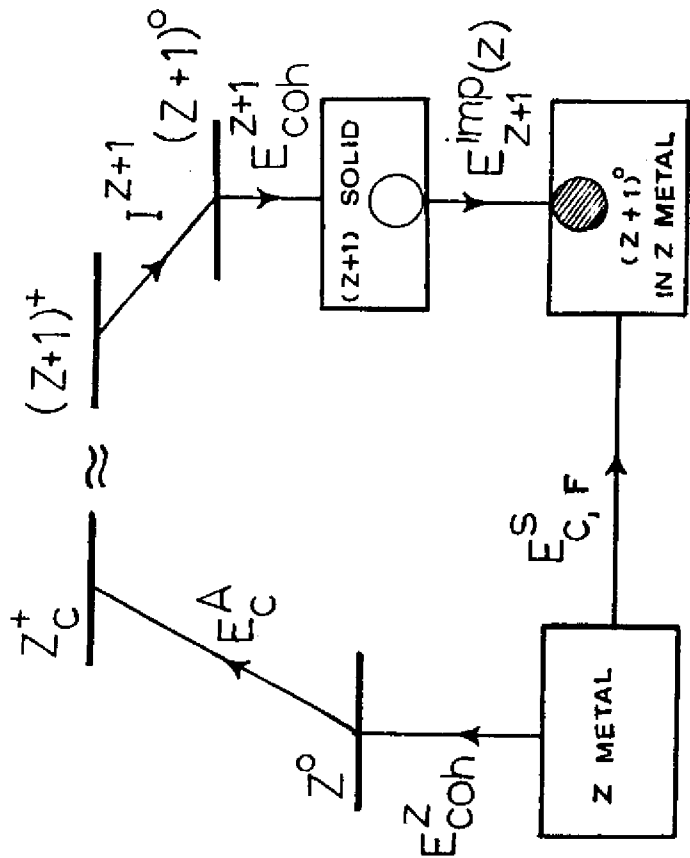


Fig. (1). The Born-Haber cycle for calculation of the  $E_{C,F}^M$  Excitation energy for the metallic solids after JM(9). Its construction is reviewed in the second section of the text.

ionized state in the sense that that the core-ionized atom Z is replaced by the valence ionized  $(Z+1)^+$  ion with the same valence electronic structure as the core-ionized Z atom. After that, this  $(Z+1)^+$  ion with a valence vacancy is neutralised by the acquisition of an electron forming the ground state of the neutral  $(Z+1)$  atom. This releases the ionization energy  $I^{Z+1}$ . Then this neutralised  $(Z+1)$  atom is embedded into the standard solid yielding the cohesive energy  $E_{coh}^{Z+1}$ . Finally one of these  $(Z+1)$  metallic sites is implanted substitutionally into a Z solid. The energy involved in this last step is the impurity heat of solution  $E_{z+1}^{imp}(z)$ . In this way one arrives at the final state which has a  $(Z+1)$  impurity site in the otherwise perfect Z solid. This final situation is equivalent to the thermal excitation of the core electron from an atom at a specific site of Z solid up to the fermi level. It should, however, be mentioned that photoexcitation is a vertical process and thus this core-ionization energy will in principle be a lower limit to the actual experimental value.

Thus the energy balance of the cycle,

$$E_{coh}^Z + E_C^A - I^{Z+1} - E_{coh}^{Z+1} + E_{z+1}^{imp}(z)$$

can be meaningfully taken as an evaluation of the core-binding energy in the solid,  $E_{C,F}^M$  (here the subscript F stands for relative to the fermi level). The sought core-level binding energy shift,

$$E_C = E_C^A - E_{C,F}^S = I^{Z+1} + E_{coh}^{Z+1} - E_{coh}^Z - E_{z+1}^{imp}(z) \quad (2)$$

is then expressed in terms of easily accessible experimental quantities with the exception of  $E_{z+1}^{imp}(z)$ . This quantity  $E_{z+1}^{imp}(z)$

could in principle be obtained from the experiment but very little data is available in the literature. Therefore some other scheme has to be used for the evaluating of this quantity. For the metallic solid Miedema's<sup>(9)</sup> scheme seems more preferable. The above eqn. (2) is the exact expression of the excitation of the core electron from an atom at a specific site of the solid to the fermi level. This is the scheme used by JM to evaluate the core-level binding energy shifts for the metallic elements.

## 2.2. APPLICATION TO SEMICONDUCTORS

In the case of the metallic solids, the previous description with the complete screening picture of the core hole is indeed appropriate with the photoemission experiment, by which  $E_{c,F}^M$  is usually measured, because the core-ionized ion is left completely screened by the electrons at the fermi level. The question then arises to what extent a similar screening picture is applicable to semiconductors and insulators.

One essential complication associated with the photoemission threshold for the nonmetals is that in these elements ordinary photoemission does not leave behind a neutral core-hole since the screening is incomplete - a field  $e^2/\epsilon_0 r$  remains at large distances. Hence perfect screening for the core-hole cannot be expected and this final state is not exactly the same as the neutral impurity implied in the above scheme.

Our observation is that the above difficulty can be remedied by alternatively measuring the core-level binding energy for the semiconductor by the core-to-conduction photoabsorption threshold, the so called "core-exciton", rather than the ordinary photoemission threshold, where the final electron is removed. In an optical experiment the photoexcited electron, subject to the screened coulomb potential of the very localized hole, should reach a final state closely resembling that of an electron in the field of a donor impurity<sup>(8,12)</sup>. The excitation of such bound exciton states is schematically shown in Fig. (2). In this way the ejected electron goes into the first available bound state

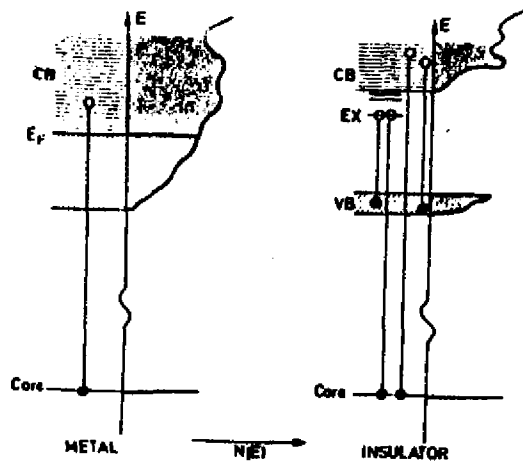


Fig. (2). The excitation of bound exciton states in metals and insulators. The density of states  $N(E)$  is indicated towards the right.  $E_F$  = Fermi energy. CB = conduction band. VB = valence band.  $E_x$ , exciton.

about the core-hole and the screening becomes complete at some distance larger than the binding radius. This modification allows us to consider the initial state before core ionization as the perfect semiconductor and the final state after core ionization as the neutral  $Z+1$  impurity site in an otherwise perfect semiconductor. We can then replace the core-ionized  $Z$  atom (with the core-hole-electron bound state) by the core of the  $Z+1$  atom. This  $Z+1$  neutral impurity inside the  $Z$  semiconductor is now clearly a very similar object to previous case and in this way JM's scheme becomes applicable. We will then regard  $E_{c,exciton}^S$  as the excitation energy of the core electron to the core exciton level in the semiconductor.

The new Born-Haber cycle appropriate to semiconductors is illustrated again in Fig. (3). The steps involved in the cycle are the same as before and thus we are led to the following final expression for the core-level binding energy shift for the semiconductor,

$$\Delta E_c = E_c^A - E_{c,exciton}^S = I^{z+1} + E_{coh}^{z+1} - E_{coh}^z - E_{z+1}^{imp}(z) \quad (3)$$

There exist experimental photoabsorption yield spectra for some semiconductors from which we can locate almost accurately the position of  $E_c^S$  relative to the core - exciton level. Thus, provided  $E_{z+1}^{imp}(z)$  for semiconductor can be evaluated, we should be able to evaluate the core-level binding energy shifts for the group IV semiconductors and semimetals and make a direct comparison with the experimental data as well.



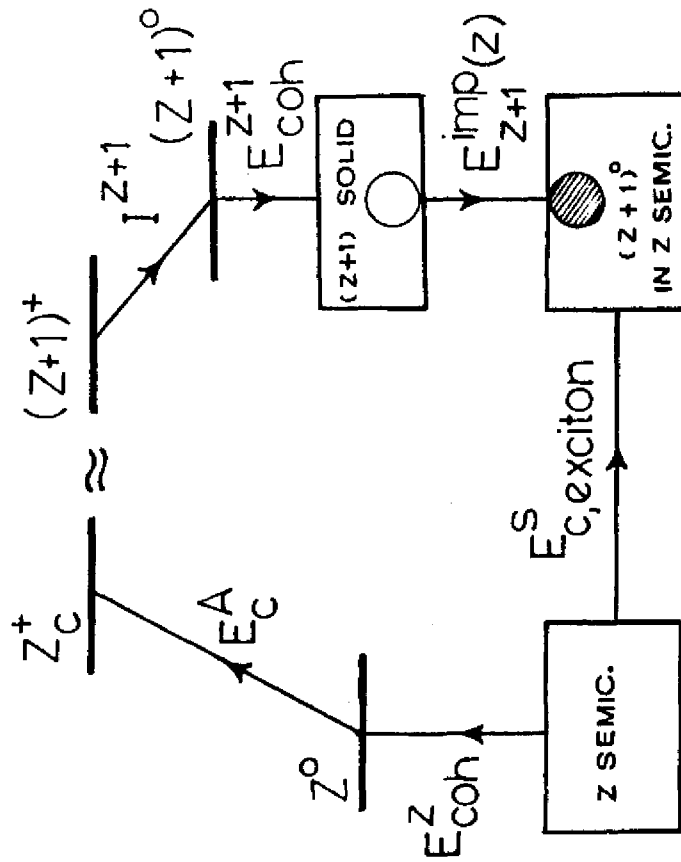


Fig.(3). The modified Born-Haber cycle for calculation of  $E_{C,exciton}^S$ , excitation energy of core electron to the exciton level for semiconductors.

The experimental core-level binding energy shifts, in principle, can be obtained from the difference of experimental core binding energy of the free atom and the experimental binding energy of the same atomic core level from the solid. However due to the lack of experimental core-level binding energies for free atom it has been common to obtain the experimental core-level binding energy shifts by using theoretical or semiempirical atomic core binding energies together with measured core levels for the solids<sup>(13)</sup>.

In the next section we will consider two alternative methods for the evaluation of the impurity heat of solution  $E_{z+1}^{imp}$  associated with the implantation of  $Z+1$  impurity into a  $Z$  semiconductor.

### 3 THE HEAT OF SOLUTION $E_{z+1}^{\text{imp}}(z)$

#### 3.1 $E_{z+1}^{\text{imp}}(z)$ BY SIMPLIFIED HYBRID CLUSTER MODEL

Semiconductors are held together by strong, directional, covalent bonding among nearest neighbour atoms. Silicon, germanium and  $\alpha$ -tin have the diamond structure with atoms joined to four nearest neighbours at tetrahedral angle ( $109^\circ 28'$ ). According to the theory of hybrid bond orbitals the s-orbital and three p-orbitals of each atom are hybridized to form four tetrahedral  $sp^3$  hybrid orbitals strongly overlapping with adjacent atoms in the tetrahedral direction. The electrons are considered to be localized in distinct bonds.

The most important advantage of using the hybrid cluster model is that it allows us to think of a chemical bond in terms of a 2-electron wave function built up from particular orbitals of the two atomic centers involved. To evaluate  $E_{z+1}^{\text{imp}}(z)$  by making use of the simplified hybrid cluster with Huckel technique, we first assume that this quantity is equivalent to the change in local chemical bond energy due to the replacing of central z-atom by a (z+1)-atom in  $sp^3$  hybrid cluster.

In the following we present two calculations of  $E_{z+1}^{\text{imp}}(z)$ , for diamond, silicon, germanium,  $\alpha$ -tin ( $sp^3$  hybrid cluster), and graphite ( $sp^2$  hybrid cluster).

#### 3.1(a) $E_{z+1}^{\text{imp}}(z)$ FOR DIAMOND-LIKE STRUCTURE

We consider a tetrahedral  $sp^3$  hybrid cluster model for diamond-like structure in which  $sp^3$  hybrid orbitals of z-atom are directed onto the central atom as shown in Fig. (4). At first we consider the central atom as a z-atom and later we will replace this z-atom by (z+1)-atom. The orthonormal atomic orbitals on each atom at the four corners A, B, C and D of the tetrahedral cluster are given by,

$$\begin{aligned}\Psi_1 &= 1/2 (s^A - \sqrt{3}p_z^A) \\ \Psi_2 &= 1/2 (s^B - \sqrt{3}/3 p_x^B + \sqrt{3} p_z^B) \\ \Psi_3 &= 1/2 (s^C + \sqrt{2}/3 p_x^C + \sqrt{3} p_z^C - \sqrt{2} p_y^C) \\ \Psi_4 &= 1/2 (s^D + \sqrt{2}/3 p_x^D + \sqrt{3} p_z^D + \sqrt{2} p_y^D)\end{aligned}\quad (4)$$

Here s and p are the atomic orbitals where p-orbitals are pointing along the bond direction. Since the tetrahedral cluster has  $T_d$  symmetry we can construct the eigen-functions  $\Psi_{T_2}$  and  $\Psi_{T_2^*}$  for the linear combination of above atomic orbitals as follows.

$$\begin{aligned}\Psi_{T_2} &= 1/2 (\Psi_1 + \Psi_2 + \Psi_3 + \Psi_4) \\ \Psi_{T_2^*} &= 1/2\sqrt{3} (3\Psi_1 - \Psi_2 - \Psi_3 - \Psi_4)\end{aligned}\quad (5)$$

For the central atom we assign s and p wave functions, namely  $\phi_s^o$ ,  $\phi_{px}^o$ ,  $\phi_{py}^o$ ,  $\phi_{pz}^o$ , with

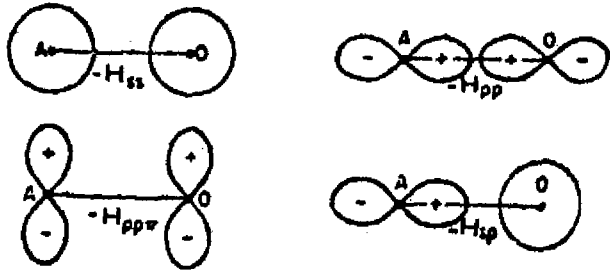
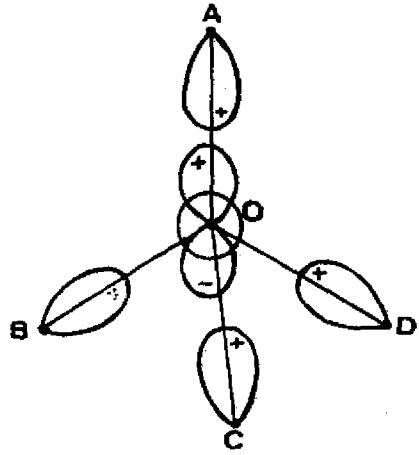


Fig.(4). (a) Schematic tetrahedral  $sp^3$  hybrid-cluster bond orbitals for diamond-like structure.

(b) Schematic atomic orbitals and the definition of the matrix elements  $H_{ss}$ ,  $H_{sp}$ ,  $H_{pp}$ , and  $H_{pp\pi}$ . The positions of the atoms are indicated by O (the central atom of the hybrid-cluster) and A (the atoms at the corner of the hybrid-cluster).

eigen-values  $\epsilon_s$  and  $\epsilon_p$  which are taken as atomic s and p energy values for the free z-atom.

We obtain the eigen-energy  $E_{\Gamma_1}(z)$  by solving the usual eigen-value problem between  $\Psi_{\Gamma_1}$  and  $\Phi_s^0$ . The final result is

$$E_{\Gamma_1}(z) = 1/2(\epsilon_h + \epsilon_s) - 1/2\sqrt{(\epsilon_h - \epsilon_s)^2 + 4V_1^2} \quad (6)$$

Here we use  $\epsilon_h = \langle \Psi_{\Gamma_1} | H | \Psi_{\Gamma_1} \rangle = \frac{\epsilon_s + 3\epsilon_p}{4}$  (the eigen-energy of  $\Psi_{\Gamma_1}$ )  
 $\epsilon_s = \langle \Phi_s^0 | H | \Phi_s^0 \rangle$ ,  $V_1 = \langle \Psi_{\Gamma_1} | H | \Phi_s^0 \rangle$  and H is the Hamiltonian for the total system<sup>(14)</sup>.

Similarly, by solving the eigen-value problem between  $\Psi_{\Gamma_2}$  and  $\Phi_p^0$  as well, we obtain the eigen-energy as follows.

$$E_{\Gamma_2}(z) = 1/2(\epsilon_h + \epsilon_p) - 1/2\sqrt{(\epsilon_h - \epsilon_p)^2 + 4V_2^2} \quad (7)$$

where  $\epsilon_p = \langle \Phi_p^0 | H | \Phi_p^0 \rangle$  and  $V_2 = \langle \Psi_{\Gamma_2} | H | \Phi_p^0 \rangle$ .

The values of  $V_1$  and  $V_2$  can be obtained explicitly as,

$$\begin{aligned} V_1 &= \langle \Psi_{\Gamma_1} | H | \Phi_s^0 \rangle \\ &= 1/2 \langle \Psi_1 + \Psi_2 + \Psi_3 + \Psi_4 | H | \Phi_s^0 \rangle \\ &= H_{ss} - \sqrt{3} H_{sp} \end{aligned} \quad (8)$$

$$\begin{aligned}
V_2 &= \langle \Psi_{\Gamma_5}^A | H | \phi_{pz}^0 \rangle \\
&= 1/2\sqrt{3} \langle 3\Psi_1 - \Psi_2 - \Psi_3 - \Psi_4 | H | \phi_{pz}^0 \rangle \\
&= -1/\sqrt{3} H_{sp} - 7/9 H_{pp\sigma} - 2/9 H_{pp\pi} \quad (9)
\end{aligned}$$

Here  $H_{ss}$ ,  $H_{sp}$ ,  $H_{pp\sigma}$  and  $H_{pp\pi}$  denote respectively the following matrix elements,

$$\begin{aligned}
H_{ss} &= \langle s^A | H | \phi_s^0 \rangle \\
H_{sp} &= \langle p_z^A | H | \phi_s^0 \rangle \\
H_{pp\sigma} &= \langle p_z^A | H | \phi_{pz}^0 \rangle_{\sigma} \\
H_{pp\pi} &= \langle p_z^A | H | \phi_{pz}^0 \rangle_{\pi}
\end{aligned}$$

Now we replace the z-atom by (z+1)-atom at the centre of the cluster. The eigen value  $\epsilon_h$  will change into  $(\epsilon'_h + \epsilon_{\text{coul}})$ , where  $\epsilon'_h = \frac{\epsilon'_s + 3\epsilon'_p}{4}$ , and  $\epsilon'_s$  and  $\epsilon'_p$  are atomic s and p energy values of (z+1)-atom respectively.  $\epsilon_{\text{coul}}$  is the screened coulomb potential due to the extra electron at the central atom which is estimated by,

$$\epsilon_{\text{coul}} = \frac{e^2}{R} e^{-k_{FT}R} \quad (10)$$

Here R is taken to be the nearest neighbour distance and  $k_{FT}$  is the Fermi-Thomas wave vector given by <sup>(15)</sup>,

$$k_{FT} = \sqrt{3} \frac{w_p}{v_F} = \sqrt{3} \frac{(4\pi n e^2/m)^{\frac{1}{2}}}{(3\pi^2 n)^{1/3}/m} \quad (11)$$

With (z+1)-atom at the central site we again calculate the energy eigen-values  $E_{\Gamma_1}(z+1)$  and  $E_{\Gamma_5}(z+1)$ , following the same procedure as above, and the final results are as follows.

$$\begin{aligned}
E_{\Gamma_1}(z+1) &= 1/2 (\epsilon'_h + \epsilon_{\text{coul}} + \epsilon'_s) - 1/2 \sqrt{(\epsilon'_h + \epsilon_{\text{coul}} - \epsilon'_s)^2 + 4V_1^2} \\
E_{\Gamma_5}(z+1) &= 1/2 (\epsilon'_h + \epsilon_{\text{coul}} + \epsilon'_p) - 1/2 \sqrt{(\epsilon'_h + \epsilon_{\text{coul}} - \epsilon'_p)^2 + 4V_2^2} \quad (12)
\end{aligned}$$

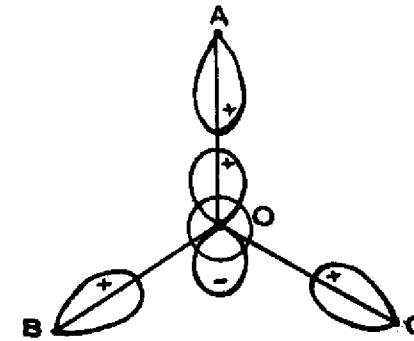
Here we have neglected the difference in orbital overlapping from (z+1)-atom to z-atom and also taken  $V_1$  and  $V_2$  for (z+1) atom as the same for the corresponding values of the z-atom.

To evaluate  $E_{z+1}^{\text{imp}}(z)$ , we consider the following picture. For the initial state, we assume that  $sp^3$  hybrid cluster of z-atoms is a host and a free (z+1)-atom with 5 valence electrons is a guest outside. For the final state, we replace central z-atom by (z+1)-atom in the cluster. (putting one electron on  $E_{\Gamma_5}^+$  level) and place the free z-atom with 4 valence electrons outside the cluster. Then we can estimate  $E_{z+1}^{\text{imp}}(z)$ , which is equivalent to the change in local chemical bonding energy caused by the replacement of z-atom by (z+1)-atom at the center of the z-hybrid-cluster, as follows.

$$\begin{aligned}
E_{z+1}^{\text{imp}}(z) &= \left\{ 2 [E_{\Gamma_1}(z+1) + 3E_{\Gamma_5}(z+1)] + E_{\Gamma_5}^+(z+1) + 2\epsilon_s(z) + 2\epsilon_p(z) \right\} - \\
&\quad - \left\{ 2 [E_{\Gamma_1}(z) + 3E_{\Gamma_5}(z)] + 2\epsilon_s(z+1) + 3\epsilon_p(z+1) \right\} \quad (13)
\end{aligned}$$

The first bracket in eqn.(13) is the total atomic energy for the final state and the second bracket is that for the initial state. We have placed the extra electron from (z+1)-atom in the lowest conduction band  $E_{V_5}^+(z+1)$ , in the final state, to make sure of the complete screening.

To evaluate  $E_{z+1}^{imp}(z)$  from eqn.(13), we make use of the atomic  $\epsilon_s$  and  $\epsilon$  energy values from Clementi's H-F calculations <sup>(16)</sup>P of ground-state atoms. The matrix elements  $H_{ss}$ ,  $H_{sp}$ ,  $H_{pp\sigma}$ , and  $H_{pp\pi}$  are extracted from Harrison's work. They are obtained by fitting the energy bands of group IV semiconductors. <sup>(17)</sup>



### 3.1(b) $E_{z+1}^{imp}(z)$ FOR GRAPHITE

Graphite is a layer compound and therefore we consider  $sp^2$  hybrid cluster model with three  $sp^2$  hybrid orbitals directed towards the central atom on the same layer as shown in Fig.(5). The orthonormal atomic orbitals are then given by,

$$\begin{aligned} \Psi_1 &= \frac{1}{\sqrt{3}} (s^A - \sqrt{3} p_y^A) \\ \Psi_2 &= \frac{1}{\sqrt{3}} (s^B + \sqrt{3/2} p_x^B + \sqrt{2} p_y^B) \\ \Psi_3 &= \frac{1}{\sqrt{3}} (s^C - \sqrt{3/2} p_x^C + \sqrt{2} p_y^C) \end{aligned} \quad (14)$$

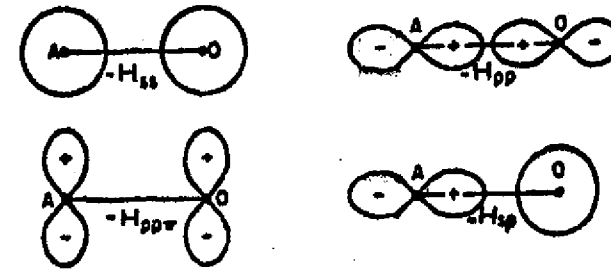


Fig.(5). Schematic  $sp^2$  hybrid-cluster for layer structure of graphite.

Since this cluster has  $C_{3v}$  symmetry, we construct the eigen function  $\Psi_{\Gamma_1}$  and  $\Psi_{\Gamma_3}$  as the following linear combinations of  $\Psi_1, \Psi_2,$  and  $\Psi_3$ .

$$\begin{aligned}\Psi_{\Gamma_1} &= 1/\sqrt{3} (\Psi_1 + \Psi_2 + \Psi_3) \\ \Psi_{\Gamma_3} &= 1/\sqrt{6} (2\Psi_1 - \Psi_2 - \Psi_3)\end{aligned}\quad (15)$$

We can obtain the energy eigen-values  $E_{\Gamma_1}(z), E_{\Gamma_2}(z), E_{\Gamma_1}(z+1)$  and  $E_{\Gamma_2}(z+1)$  for the  $\sigma$ -bond following the same procedure as for the diamond-like structure above. The values of  $V_1$  and  $V_2$  for the present case are,

$$\begin{aligned}V_1 &= H_{ss} - \sqrt{2} H_{sp} \\ V_2 &= -1/\sqrt{2} H_{sp} - 3/4 H_{pp\sigma} - 1/4 H_{pp\pi}\end{aligned}\quad (16)$$

Finally the relation for  $E_{z+1}^{imp}(z)$  for graphite can be obtained as follows.

$$\begin{aligned}E_{z+1}^{imp}(z) &= \left\{ 2E_{\Gamma_1}(z+1) + 4E_{\Gamma_3}(z+1) + 2E_{\pi_3}(z+1) + 2\epsilon_s(z) + 2\epsilon_p(z) \right\} - \\ &\quad - \left\{ 2E_{\Gamma_1}(z) + 4E_{\Gamma_3}(z) + 2E_{\pi_3}(z) + 2\epsilon_s(z+1) + 2\epsilon_p(z+1) \right\}\end{aligned}\quad (17)$$

The matrix elements  $H_{ss}, H_{sp}, H_{pp\sigma}$  and  $H_{pp\pi}$  are taken from the energy band calculations of Bassani et al.<sup>(18)</sup> The values of  $E_{\pi_3}(z) = -2.3 - \phi$  and  $E_{\pi_3}(z+1) = -\Delta\epsilon_p - E_{\pi_3}(z)$ , which are the eigen-energies of  $\pi$ -bonds for graphite, are taken from the band structure after Painter

and Ellis<sup>(19)</sup>.

In Table (1) we have collected all the matrix elements  $H_{ss}, H_{sp}, H_{pp\sigma}$  &  $H_{pp\pi}$  and the results of  $V_1$  and  $V_2$  extracted from them. In Table (2) the eigen-energy values of atomic s and p orbitals together with eigen-energy values of the hybrid-clusters for Z-semiconductors are given.  $\epsilon_{coul}$ , the screened coulomb potential, and the final results of  $E_{z+1}^{imp}(z)$  are also collected in the same Table.

To check the reliability of our calculated eigen-energy values, we extract cohesive energies out of these. We find that the extracted cohesive energies differ from the experimental values by large amounts. This is shown in Table (3). This indicates that our calculated  $E_{z+1}^{imp}(z)$  values will also be rather large to use in eqn. (3). However, in our view, a rescaled value of  $E_{z+1}^{imp}(z)$  by using the calculated cohesive energy and the experimental value will be of more practical use. Friedel<sup>(20)</sup>, who also has obtained a large difference between his calculated cohesive energies and the experimental values, has pointed out that relative values still make physical sense. Thus we choose to make use of the rescaled value  $E_{z+1}^{imp'}(z)$  for our calculation of core-level shift. With this rescaling we modify eqn. (3) as,

$$E_{z+1}^{imp'}(z) = E_{coh}^{exp} / E_{coh}^{th} \times E_{z+1}^{imp}(z)\quad (18.a)$$

$$\Delta E_c = I^{z+1} + E_{coh}^{z+1} - E_{coh}^z - E_{z+1}^{imp'}(z)\quad (18)$$

Here  $E_{coh}^{th}$  refers to the calculated cohesive energy for Z semiconductor obtained from our cluster model. As Table (3) shows the scaling factor,  $h = E_{coh}^{exp} / E_{coh}^{th}$ , is as small as 0.3 in C and grows to 0.5 in Si.

Table (1)

	$H_{ss}$	$H_{sp}$	$H_{pp}$	$H_{pp\kappa}$	$V_1$	$V_2$
C(diamond)	-2.96	4.11	2.38	-1.32	-10.08	-3.94
C(graphite)	-2.86	6.12	3.26	-1.90	-13.44	-5.65
Si	-1.44	1.97	0.17	-0.62	-4.86	-1.13
Ge	-1.32	1.03	0.08	-0.67	-4.83	-1.09
$\alpha$ -Sn	-1.09	1.69	0.02	-0.55	-4.03	-0.87

all values are given in eV.

	$\epsilon_s$	$\epsilon_p$	$\epsilon_{coul}$	$E_{\Gamma_1}$	$E_{\Gamma_{15,\Gamma_3}}$	$E_{\Gamma_{15,\Gamma_3}}$	$E_{z+1}^{imp}$
C(diamond)	-19.19	-11.79	0.18	-26.87	-16.76	-8.67	4.63
N	-25.71	-15.44		-31.47	-18.65	-10.61	
C(graphite)	-19.19	-11.79	0.18	-30.14	-18.44	-6.99	3.32
N	-25.71	-15.44		-34.46	-20.34	-8.92	
Si	-14.68	-8.08	0.05	-17.66	-10.31	-7.5	1.83
P	-18.94	-10.65		-21.04	-11.43	-9.0	
Ge	-15.10	-7.8	0.04	-17.91	-10.14	-7.29	2.31
As	-18.70	-10.05		-20.79	-10.96	-8.76	
$\alpha$ -Sn	-12.96	-7.21	0.02	-15.37	-9.06	-6.79	1.75
Sb	-15.83	-9.11		-17.64	-9.79	-7.94	

all values are given in eV.

Table (2)

Table (3)

	$I^{z+1}$	$E_{\text{coh}}^{z+1}$	$E_{\text{coh}}^z(\text{exp})$	$E_{\text{coh}}^z(\text{th})$	$h^{(a)}$	$E_{z+1}^{\text{imp}'}(z)$ (b)	$\Delta E_c$ (c)
C(diamond)	14.5	4.9	7.36	22.6	0.33	1.53	10.5
C(graphite)	14.5	4.9	7.37	24.2	0.30	1.01	11.0
Si	10.5	3.4	4.6	9.2	0.5	0.92	8.4
Ge	9.8	2.9	3.9	9.8	0.4	0.92	7.9
-Sn	8.6	2.7	3.1	7.9	0.39	0.69	7.5

all values are given in eV.

(a) from eqn. (18.a),  $h = E_{\text{coh}}^{z(\text{exp})} / E_{\text{coh}}^{z(\text{th})}$

(b)  $E_{z+1}^{\text{imp}'}(z) = h \times E_{z+1}^{\text{imp}}(z)$

(c) from eqn. (18).

By making use of the experimental values for  $I^{z+1}$ ,  $E_{\text{coh}}^z$  and  $E_{\text{coh}}^{z+1}$  we are thus able to calculate the core-level binding energy shift of the group IV elements from eqn. (18). The cohesive energies are taken from the tabulation by Brewer<sup>(21)</sup>. Ionization energies are taken from the atomic energy level data compiled by Moore<sup>(22)</sup>. These experimental cohesive energies together with the calculated cohesive energies are collected in Table (3). The final results of  $\Delta E_c$ , obtained from eqn. (18), are also given in the last column of the same Table.



### 3.2 $E_{z+1}^{imp}(z)$ BY SEMI-EMPIRICAL CALCULATION

An alternative way of semi-empirical evaluation for  $E_{z+1}^{imp}$  for semiconductors is found in Van Vechten's work<sup>(10)</sup>. In principle,  $E_{z+1}^{imp}(z)$  is equivalent to the excess heat of mixing  $H_m(I_x A_{1-x})$ , which in turn, is due to mixing of  $x$  concentration of  $(z+1)$ -impurity  $I$  into  $z$ -semiconductor  $A$  at the critical temperature  $T_c$ . According to Van Vechten's scheme, this quantity can be separated into two parts,

$$E_{z+1}^{imp}(z) = H_m(I_x A_{1-x}) = E_1(I_x A_{1-x}) + E_2(I_x A_{1-x}), \quad (19)$$

where the contribution  $E_1$  is the heat of mixing produced by the reduction of the various band gaps (caused by the disorder of the host semiconductor potential connected with incorporation of the impurity). The contribution  $E_2$  is due to the effect of the excess electrons (excess from the number required to exactly fill the valence bands and leave all the conduction bands empty).

Our interpretation of these two quantities, in connection with the  $(z+1)$ -approximation, is that  $E_1$  is just equivalent to the change in the energy of the chemical bonds due to the replacement of  $Z$  atom by  $Z+1$  atom in an otherwise perfect  $Z$  semiconductor whereas  $E_2$  is equivalent to extra energy required by an electron to climb from the intrinsic fermi level at mid-gap to the bottom of the conduction band.

In Van Vechten's work,  $E_1$  is obtained by the empirical relation,

$$E_1 = D(A) \cdot (E^{JM} - E^{PP}) \quad (20)$$

where  $(E^{JM} - E^{PP})$  is the difference in internal energy per electron between an idealized  $sp^3$  hybrid (PP model) semiconductor and an idealized (jellium model) metal.  $D(A)$  is an empirical factor which can be obtained in terms of various direct band gaps fitting the measured transition energies.

$E_2$  is given by the relation,

$$E_2 = I \cdot (E_f - E_v) \cdot (Z(I) - Z(A)) \quad (21)$$

where  $(E_f - E_v)$  denotes the enthalpy difference between the fermi level and the valence band edges and  $I$  is the concentration of the impurity. The crucial assumption is that the dominant ionization state of the impurity has charge  $-e(Z(I) - Z(A))$ .

Van Vechten has evaluated  $E_1$  and  $E_2$  for Si and Ge with different kinds of impurities. He has been kind enough to supply us his unpublished results.<sup>(10)</sup> The values of  $E_1$  and  $E_2$  for Si:P and Ge:As are given in Table (4). However the values for C:N and -Sn:Sb are not contained in his work.

Since  $E_2$  is expected to be equivalent to the energy required by an electron to climb up to the conduction band from the fermi level, we can estimate it as,

$$E_2 = E_{\text{cond}} - E_F - E_B \quad (22)$$

or roughly,

$$E_2 = E_{\text{gap}}/2 - E_B$$

where  $E_B$  is some small impurity-like binding energy. As shown in Table(4), one can find that  $E_2$  is somewhat smaller than  $E_{\text{gap}}/2$  and also  $E_1$  is small (of the order of half an electron volt). This situation suggests that by first assuming  $E_2 = E_{\text{gap}}/2$ , and then neglecting  $E_1$ , might not be too bad for C:N and  $\alpha$ -Sn:Sb as well.

This is the choice we have made for the alternative semi-empirical evaluations of  $E_{z+1}^{\text{imp}}(z)$  for the group IV elements. Corresponding core-level binding energy shifts are obtained from eqn.(3) by making use of above quantities together with the experimental values of ionization energies and cohesive energies. The results are collected in Table(4). We find that the agreement between  $\Delta E_c$  obtained from both alternative methods are quite satisfactory.

In the following section we will give an account on the comparison we make between the calculated  $\Delta E_c$  and available experimental data.

Table (4)

	$I^{z+1}$	$E_{\text{coh}}^z$	$E_{\text{coh}}^{z+1}$	$E_1$	$E_2$	$E_{z+1}^{\text{imp}}(z)$	$\Delta E_c^{(c)}$
C(diamond)	14.5	7.36	4.9	-	2.7 <sup>(a)</sup>	2.7	9.6
C(graphite)	14.5	7.37	4.9	-	0 <sup>(a)</sup>	0	12.1
Si	10.5	4.6	3.4	0.2 <sup>(b)</sup>	0.6 <sup>(a)</sup> (0.22) <sup>(b)</sup>	0.8 <sup>(c)</sup>	8.5
Ge	9.8	3.9	2.9	0.7 <sup>(b)</sup>	0.4 <sup>(a)</sup> (0.1) <sup>(b)</sup>	1.1 <sup>(c)</sup>	7.8
$\alpha$ -Sn	8.6	3.1	2.7	-	0 <sup>(a)</sup>	0	8.2

(a) Assumed to be  $\frac{1}{2}E_{\text{gap}}(T=0)$

(b) Calculated at  $T = T_{\text{critical}}$  by J. Van Vechten(13)

(c) From eqn.(3)

4 CORE LEVEL BINDING ENERGIES OF GROUP IV  
ATOMS AND SOLIDS

Experimentally, it turns out that not much is known about the core-level binding energies of the free atom  $E_c^A$ . There are few data available for some simple metals but they are usually one or few of the inner ionizations that have been measured. No experimental data of core-level binding energies of group IV semiconductors and semimetals have been reported so far. Therefore in such a situation it might seem reasonable to rely on calculated core binding energies instead. One possibility is to derive the atomic core-level binding energy from Hartree-Fock-Slater calculations as carried out by Huang et al<sup>(23)</sup>. We denote this energy by  $E_c^A(H)$ . Another possibility is to follow the method of Johansson et al<sup>(7)</sup> to get quasi-experimental atomic core-level binding energy by summing the experimental ionization potential energies. We label this energy by  $E_c^A(JM)$ . We observe that the agreement between these two atomic core-level binding energies are rather good in general. For  $2p_{3/2}$  core level of Si atom we find that  $E_c^A(H)=107.6$  eV and  $E_c^A(JM)=108.9$ eV where the discrepancy being about 1% only. In the case of the  $3d_{5/2}$  core level of Ge atom  $E_c^A(H)=35.8$ eV whereas  $E_c^A(JM)=37.9$ eV. For  $4d_{5/2}$  core level of  $\alpha$ -Sn atom we find that  $E_c^A(H)=30.8$ eV and  $E_c^A(JM)=32.4$ eV. Finally we find that for  $1s_{1/2}$  core level of C atom  $E_c^A(H)=296.8$ eV. This atomic core binding energy is not available from JM's method. These  $E_c^A$  values are collected in Table(5).

We make two distinctions for the experimental core-level binding energy shift in order to make a comparison with our calculated shift. The calculated atomic core-level binding energy  $E_c^A(H)$  combined with measured energy for the solid will be called "pseudo-experimental" core-level binding energy shift  $\Delta E_c(PE)$ . On the other hand, the quasi-experimental atomic core-level binding energy  $E_c^A(JM)$  combined with measured energy of the solid will be called "quasi-experimental" core-level binding energy shift  $\Delta E_c(QE)$ . We collect both experimental core-level binding energies, if available, in Table(5).

In general, experimental core-level binding energy relative to the core-exciton level for group IV semiconductors and semimetals can be obtained by photoabsorption measurements. However most of the core-level energies available for solids are measured by photoemission experiments, measuring with respect to the valence band or fermi level. The only core-exciton threshold directly known from the photoabsorption experiment is for  $3p_{3/2}$  core level of Si. Therefore for the remaining cases, we extract the experimental core-level binding energy relative to the core-exciton level, namely  $E_{c,exciton}^s$  by adding up the core-valence energy difference known from the photoemission experiments and the thermal energy gap, and then subtracting  $E_B$  which is the binding energy for electron-core-hole, i.e,

$$\begin{aligned} E_{c,exciton}^s &= (E_{valence}^s - E_{core}^s) + E_{gap} - E_B \\ &= E_{core-valence}^s + E_{gap} - E_B. \end{aligned} \quad (22)$$

Table (5)

	$E_c^A(H)$	$E_c^A(JM)$	$E_{c,exc}^S$	(f) $\Delta E_c(PE)$	(g) $\Delta E_c(QE)$	(h) $\Delta E_c$	(i) $\Delta E_c$
C(diamond) ( $1s_{1/2}$ )	296.8	-	$289.2 - E_B^{(a)}$	$7.6 + E_B$	-	9.6	10.5
C(graphite) ( $1s_{1/2}$ )	296.8	-	$284.7^{(b)}$	12.1	-	12.1	11.0
Si( $2p_{3/2}$ )	107.6	108.9	$99.8^{(c)}$	7.8	9.1	8.5	8.4
Ge( $3d_{5/2}$ )	35.8	37.9	$29.8 - E_B^{(d)}$	$6.0 + E_B$	$8.1 + E_B$	7.8	7.9
$\Delta$ -Sn( $4d_{5/2}$ )	30.8	32.4	$23.7^{(e)}$	7.1	8.7	8.2	7.5

all values are given in eV.

(a) From  $E_{val} - E_c^S$  of McFeely et al (24), +  $E_{gap}$

(b) D. A. Shirley et al (25).

(c) F. C. Brown et al (26).

(d) From  $E_{val} - E_c^S$  of D. Eastman et al (28), +  $E_{gap}$ .

(e) R. A. Pollak et al (30).

(f) Obtained by subtracting column 3 from column 1.

(g) Obtained by subtracting column 3 from column 2.

(h) From eqn. (3).

(i) From eqn. (18).

First we consider the experimental core binding energy for diamond. The XPS spectrum of diamond has been investigated by McFeely and co-workers<sup>(24)</sup>. The position of the top of the valence band is located at 283.8 eV relative to C( $1s_{1/2}$ ) core level. The thermal energy gap of diamond is 5.4 eV. Assuming, at the moment,  $E_B$  as small and unknown quantity, we extract  $E_{c,exciton}^S$  for C( $1s_{1/2}$ ) level of diamond from eqn. (22) and obtain  $E_{c,exc}^S(1s_{1/2}) = (289.2 - E_B)$  eV.

Graphite is a semimetal and therefore fermi level is a good reference to locate the core-level binding energy for this element. The valence-band XPS spectrum of graphite has been investigated by Shirley et al<sup>(25)</sup> and by McFeely et al<sup>(24)</sup> as well. They reported that the  $1s_{1/2}$  core binding energy relative to the fermi level for graphite is  $E_{c,F}^S(1s_{1/2}) = 284.7$  eV.

Yield spectrum of 2p core level of pure silicon has been thoroughly investigated by Brown et al<sup>(26)</sup> and also by Eberhardt et al<sup>(27)</sup>. Their investigations give the direct measured values of  $2p_{3/2}$  core binding energy of Si relative to the core-exciton level. They reported that  $E_{c,exc}^S(2p_{3/2}) = 99.8$  eV with the excitonic binding energy  $(0.18 + 0.2)$  for Si.

The photoemission partial yield spectrum of germanium has been investigated by Eastman et al<sup>(28)</sup> and Grobman et al<sup>(29)</sup> as well. They have located the position of  $3d_{5/2}$  core level relative to the valence band at 29.1 eV with an accuracy of 0.1 eV. The thermal energy gap of Ge is 0.9 eV. Thus we extract the experimental binding energy of  $3d_{5/2}$  core

level of Ge according to eqn.(22) and obtain  $(29.8 - E_B)$  eV.

$\alpha$ -Sn is also a semimetal and therefore fermi level is again a good reference to locate the core-level binding energies. Most of the photoemission experiments are done for white tin. Pollak et al<sup>(30)</sup> have reported that  $4d_{5/2}$  core binding energy relative to the fermi level for white tin is 23.7 eV. However, Pollak suggested that  $E_{c,F}^s(4d_{5/2})$  for grey tin will not be much different from the above value<sup>(31)</sup>.

These are the experimental values of  $E_{c,exc}^s$ : we have selected for group IV semiconductors and semimetals. These values are collected in Table(5). The pseudo-experimental  $E_c^s(PE)$  and quasi-experimental  $E_c^s(QE)$  core-level binding energy shifts are then extracted and collected also in the same table for the comparison with our calculated  $\Delta E_c$  values.

We should mention the situation connected with the values of  $E_B$ , the binding energy for core-hole-electron bound state. According to the simplest model by Wannier and Mott<sup>(32)</sup> the electron is bound to the core-hole in hydrogen-like states. However, for semiconductors, there involve several corrections due to smaller dielectric constant, effective mass and exchange repulsion from the core region.<sup>(12)</sup> At present the question of how large this binding energy  $E_B$  is still under debate<sup>(33)</sup>. Thus we are not in a clear position to assign a definite value for  $E_B$ . Nevertheless, since  $E_B < 1$  eV (except possibly for diamond) we believe that the ignorance of its exact value is not fatal for our evaluations of  $\Delta E_c$ .

From the comparison of the data given in Table(5) we observe that the agreement of calculated core-level binding energy shifts  $\Delta E_c$  (calculated from eqn.(3) and eqn.(18)) and the experimental estimates  $\Delta E_c(PE)$  and  $\Delta E_c(QE)$  is generally rather good. This result clearly supports our point of view that the complete screening picture of  $(z+1)$ -impurity in the  $z$ -solid is appropriate for semiconductors as well, provided that the core-level binding energies in semiconductors are measured relative to the core-exciton level. It is the Born-Haber cycle, of course, which makes JM's scheme possible for the calculations of  $\Delta E_c$ . However, it should be noted that the scheme becomes of practical use effectively only after the introduction of the  $(z+1)$ -approximation with complete screening.

A large discrepancy between our calculated and the experimental values of  $\Delta E_c$  is found for diamond. In our calculations we have neglected  $E_B$ , the core-hole-electron binding energy. Thus we suspect that the main contribution to this discrepancy of about 2 eV might be due to  $E_B$ . It would be interesting to check experimentally whether this implied large core-exciton binding energy  $E_B$  of order 1-2 eV for diamond is indeed there.

Another possible contribution to the errors involved in our calculations of  $\Delta E_c$  might be due to the quantity  $E_{z+1}^{imp}(z)$ , the so called impurity heat of solution. In the present work we have estimated this quantity for

semiconductors by employing two alternative methods, one totally empirical and the other based on a semi-empirical cluster model. We find that the results of  $E_{z+1}^{imp}(z)$  as directly obtained from the hybrid-cluster model turns out to be rather large for practical use. However, by introducing a proper rescaling in which we consider the relative value of  $E_{z+1}^{imp}(z)$  with respect to the calculated value of cohesive binding energy from the same model we obtain physically sensible results which are also found to be in good agreement with those data obtained by the semi-empirical method. Incidentally, the results of Table (5) provide an independent calculation of  $E_{z+1}^{imp}(z)$ , another elusive quantity to evaluate from the first principles.

In our semi-empirical scheme, the main source of difference in  $\Delta E_c$  between graphite and diamond is the necessity of climbing half the thermal gap in the latter case which seems intuitively correct.

It should also be noted that though we have considered only one core level per species, the shift predicted by this model is the same for all core levels.

Our conclusion is that the Born-Haber scheme with a  $(z+1)$ -approximation is also applicable to core levels of non-metals. The main difference in this case is that the core-level binding energy must be taken with respect to the core-exciton level rather than the fermi level as in the metallic solids. This is necessary to insure complete screening of the core hole at large distances. The results of this scheme, which expresses the core-level binding energy shifts in terms of experimental quantities such as ionization

energies and cohesive energies together with semi-empirical values of impurity heat of solution, compare satisfactory with other experimental estimates of core-level binding energy shifts. We must also note that a crude order of magnitude estimate of  $\Delta E_c$  for  $z$ -element is just  $I^{z+1}$ , the ionization energy of  $(z+1)$ -element. This estimation is also valid for metals. As shown in Table(5), this rule of thumb works decently, giving also the correct trend with increasing  $z$ .

#### ACKNOWLEDGEMENT

One of the authors (S.Y.) would like to thank Professor Abdus Salam, the International Atomic Energy Agency and UNESCO for hospitality at the International Centre for Theoretical Physics, Trieste.

REFERENCES

1. "Topics in Applied Physics", vol.26; Photoemission in Solids I , General Principles, and vol.27; Case Studies, eds. M. Cardona and L. Ley, Springer Verlag, Berlin, 1975.
2. L. Ley, S. P. Kowalczyk, F. R. McFeely, R. A. Pollak and D. A. Shirley, Phys. Rev. B8(1973)2392.
3. P. H. Citrin and D. R. Hamann, Chem. Phys. Lett. 22(1973)301.
4. A. R. Williams and N. D. Lang, Phys. Rev. Lett. 40(1978)954.
5. P. H. Citrin and T. D. Thomas, J. Chem. Phys. 57(1972)4446.
6. R. E. Watson and M. L. Perlman: "Photoemission Spectroscopy" Structure and Bonding, vol.24, Springer, Berlin, Heidelberg, New York, 1975.
7. N. Mårtensson and B. Johansson, Solid State Commun. 32(1979) 791, and B. Johansson and N. Mårtensson, to be published.
8. M. A. Altarelli, J. Physique, Coll. C4.95(1978).
9. A. R. Miedema, J. Less-Common Met. 46(1976)67.
10. J. A. Van Vechten, Phys. Rev. B7(1973)1479, and to be published.
11. D. W. Davis and D. A. Shirley, J. Electron Spectroscopy 8(1976)149.
12. C. Kunz, J. Physique, Coll. C4, 39(1978)112.
13. D. A. Shirley, R. L. Martin, S. P. Kowalczyk, F. R. McFeely, and L. Ley, Phys. Rev. B15(1977)544.
14. J. C. Slater and G. F. Koster, Phys. Rev. 94(1954)1498, and see also D. W. Bullett, J. Phys. C: Solid State Phys. 8(1975)2695.
15. C. Kittel: "Introduction to Solid State Physics ", 5th ed. New York, Wiley, 1976.
16. E. Clementi and C. Roetti, Atomic data and Nuclear data Tables, vol.14(1974), Academic Press, New York and London.
17. W. A. Harrison and S. Ciraci, Phys. Rev. B10(1974)1516.
18. F. Bassani and G. P. Parravicini, Nuovo Cimento 50B(1967)95.
19. G. S. Panter and D. E. Ellis, Phys. Rev. B1(1970)4747.
20. J. Friedel, J. Physique 39(1978)651.
21. L. Brewer, LBL-3720(1975).
22. C. E. Moore, Atomic Energy Levels, U.S. Natl. Bur. Stand. Circ. No.467(U.S) Vol.I-III(1958).
23. K.N. Huang, M. Aoyagi, M. H. Chen, B. Crasemann and H. Mark, Atomic Data 18(1976)243.
24. F. R. McFeely, S. P. Kowalczyk, L. Ley, R. G. Cavell, R. A. Pollak and D. A. Shirley, Phys. Rev. B9(1974)5268.
25. D. A. Shirley, R. L. Martin, S. P. Kowalczyk, F. R. McFeely, L. Ley, Phys. Rev. B15(1977)544.
26. F. C. Brown and O. D. Rustigi, Phys. Rev. Lett.28(1972)274.
27. W. Eberhardt, G. Kalkaffen, C. Kunz, D. Aspnes, M. Cardona, Phys. Stat. Sol. 88(1978)135.
28. D. E. Eastman and J. L. Freeouf, Phys. Rev. Lett.33(1974) 1601.

29. W. D. Grobman, D. E. Eastman and J. L. Freeouf, *phys. Rev. B*12(1975)4405.
30. R. A. Pollak, S. P. Kowalczyk, L. Ley, D. A. Shirley, *Phys. Rev. Lett.* 29(1972)274.
31. R. A. Pollak, private communication.
32. R. S. Knox: *Solid State Phys. Suppl.* 5(1963)7.
33. F. Bassani, to be published.

- IC/81/3 RAJ K. GUPTA, RAM RAJ and S.B. KHADKIKAR - Proximity potential and the surface energy part of the microscopic nucleus-nucleus interaction with Skyrme force.
- IC/81/9 E.W. MIELKE - Outline of a non-linear, relativistic quantum mechanics of extended particles.
- IC/81/10 L. FONDA and N. MANKOC-BORSTNIK - On quantum quadrupole radiation.
- IC/81/20 N.S. CRAIGIE, V. ROBERTO and D. WHOULD - Gluon helicity distributions from hyperon productions in proton-proton collisions.
- IC/81/21 QING CHENGRU and QIN DANHUA - A discussion of the relativistic equal-time equation.
- IC/81/22 F. CRISCIANI, G.C. GHIRARDI, A. RIMINI and T. WEBER - Quantum limitations for spin measurements on systems of arbitrary spin.
- IC/81/23 S.C. LIM - Stochastic quantisation of Proca field.
- IC/81/24 INT.REP.\* W. MECKLENBURG - On the zero modes of the internal Dirac operator in Kaluza-Klein theories.
- IC/81/25 INT.REP.\* SUN HONG-ZHON and HAN QI-ZHI - On the irreducible representations of the simple Lie group II - The tensor basis for the infinitesimal generators of the exceptional groups.
- IC/81/26 ZHANG YUAN-ZHONG - On the possibility for a fourth test of general relativity in Earth's gravitational field.
- IC/81/27 INT.REP.\* A.N. PANDEY, Y. KUMAR, U.P. VERMA and D.R. SINGH - Molecular properties of a few organic molecules.
- IC/81/28 E. GAVA, R. JENGO and C. OMERO - On the instanton effect in the finite temperature Yang-Mills theory and in the nonlinear  $\phi$ -model.
- IC/81/30 INT.REP.\* G. PASTORE, G. SENATORE and M.P. TOSI - Electric resistivity and structure of liquid alkali metals and alloys as electron-ion plasmas.
- IC/81/31 L. MIZRACHI - Duality transformation of a spontaneously broken gauge field.
- IC/81/32 ZHANG YUAN-ZHONG - The approximate solution with torsion for a charged particle in a gauge theory of gravitation.
- IC/81/33 INT.REP.\* W. MECKLENBURG - Massive photons and the equivalence principle.
- IC/81/34 INT.REP.\* K. TAHIR SHAH - Metric and topology on a non-standard real line and non-standard space-time.
- IC/81/35 INT.REP.\* H. PRAKASH and N. CHANDRA - Unpolarized state of light revisited.
- IC/81/36 INT.REP.\* A.N. SINGH and R.S. PRASAD - Molecular Rydberg transitions in  $C_2H_4$ ,  $HCOOH$  and  $HCOOH_2$ .



IC/81/37 H. PRAKASH - Definition and density operator for unpolarized fermion state.  
INT.REP.\*

IC/81/38 H.R. DALAFI - Microscopic description of double back-bending in <sup>168</sup>Er.

IC/81/39 B.G. SIDHARTH - Bound state wave functions of singular and transitional  
INT.REP.\* potentials.

IC/81/40 J.A. MAGPANTAY - On the non-existence of extended physical states in the  
Schwinger model.

IC/81/41 B.G. SIDHARTH - A recurrence relation for the phase-shifts of exponential  
and Yukawa potentials.

IC/81/42 M.P. TOSI and N.H. MARCH - Liquid direct correlation function, singlet  
INT.REP.\* densities and the theory of freezing.

IC/81/43 M.P. TOSI and N.H. MARCH - Theory of freezing of alkali halides and binary  
INT.REP.\* alloys.

IC/81/44 M.P. TOSI and N.H. MARCH - Freezing of ionic melts into super ionic phase.  
INT.REP.\*

IC/81/45 B.G. SIDHARTH - Large  $\lambda$  behaviour of the phase-shifts.  
INT.REP.\*

IC/81/46 G. CAMPAGNOLI and E. TOSATTI - Self-consistent electronic structure of a  
model stage-1 graphite acceptor intercalate.

IC/81/47 E. MAHDAVI-HEZAVAH - Renormalization effects in the SU(16) maximally gauged  
INT.REP.\* theory.

IC/81/48 S.C. LIM - Stochastic massless fields I. Integer spin.

IC/81/49 G. ALBERI and Z. BAJZER - Off-shell dominance in rescattering effects for  
antiproton deuteron annihilation.

IC/81/50 K. TAHIR SHAH - Self-organisation through random input by biological and  
INT.REP.\* machine systems - the pre-cognition subsystem.

IC/81/51 P. P. SRIVASTAVA - Instanton and Meron solutions for generalized  $CP^{n-1}$  model.  
INT.REP.\*

IC/81/52 G. PASTORE, G. SENATORE and M.P. TOSI - Short-range correlations in multi-  
INT.REP.\* component plasmas.

IC/81/53 L. FONDA - General theory of the ionization of an atom by an electrostatic  
field.

IC/81/54 R. d'AURIA, P. FRÉ and T. REGGE - Group manifold approach to gravity and  
supergravity theories.

IC/81/55 L. MASPERI and C. OMERO - Variational approach for the N-state spin and  
gauge Potts model.

45

IC/81/56 S. NARISON - QCD sum rules for the light quarks vacuum condensate.

IC/81/57 N.S. CRAIGIE - Spin physics at short distances as a means of studying QCD.

IC/81/58 E. SOKATCHEV - Irreducibility conditions for extended superfields.

IC/81/59 J. LUKIERSKI and L. RYTEL - Geometric origin of central charges.

IC/81/60 G. ALDÁZABAL, D. BOYANOVSKY, VERA L.V. BALTAR, L. MASPERI and C. OMERO  
Simple renormalization groups and mean-field methods for Z(N) spin models.

IC/81/61 ABDUS SALAM - Gauge interactions, elementarity and superunification.

IC/81/62 J. MAGPANTAY, C. MUKKU and W.A. SAYED - Temperature dependence of critical  
INT.REP.\* magnetic fields for the Abelian Higgs model.

IC/81/63 RAJ K. GUPTA, NEELAM MALHOTRA and R. AROUMOGAME - Role of proximity forces  
in fragmentation potentials for central and oriental heavy-ion collisions.

IC/81/64 Ch. OBCEMEA, P.FROELICH and E.J. BRÁNDAS - Generalized virial relations and  
the theory of subdynamics.

IC/81/65 W. MECKLENBURG - Attempts at a geometrical understanding of Higgs fields.  
INT.REP.\*

IC/81/66 N. KUMAR and A.M. JAYANNAVAR - Frequency and temperature dependent mobility  
of a charged carrier on randomly interrupted strand.

IC/81/67 N.S. CRAIGIE - On the hadronic problem in QCD.

IC/81/68 M.P. DAS - Electron structure calculations for heavy atoms: A local density  
INT.REP.\* approach.

IC/81/69 M.H.A. HASSAN and I.A. ELTAYEB - On the topographic coupling at the core  
INT.REP.\* mantle interface.

IC/81/70 R. HOJMAN and A. SMAILAGIC - Exact solutions for strong gravity in  
generalized metrics.

IC/81/71 B.K. AGARWAL - Electromagnetic form factor for a composite proton.  
INT.REP.\*

IC/81/72 J. BLANK, M. HAVLICEK, M. BEDNAR and W. LASSNER - Canonical representations  
of the Lie superalgebra  $Osp(1,4)$ .

IC/81/73 F.F. GRINSTEIN - Padé approximants and the calculation of spectral functions  
INT.REP.\* of solids.

IC/81/74 I.A. ELTAYEB - Hydromagnetic stability of the Kennedy-Higgins model of the  
INT.REP.\* Earth's core.

IC/81/75 S. RANDJBAR-DAEMI - A recursive formula for the evaluation of  $\langle \psi_{\mu\nu}^T(x) \psi \rangle$   
and its application in the semiclassical theory of gravity.

IC/81/76 P. BALLONE, G. SENATORE and M.P. TOSI - Coexistence of vapour-like and  
INT.REP.\* liquid-like phases for the classical plasma model.

IC/81/77 K.C. MATHUR, G.P. GUPTA and R.S. PUNDIR - Reduction of the Glauber amplitude  
INT.REP.\* for electron impact rotational excitation of quadrupolar molecular ions.

IC/81/78 N. KUMAR and A.M. JAYANNAVAR - A note on the effective medium theory of  
INT.REP.\* randomly resistive-reactive medium.

46

- IC/81/79 S.N. PANDEY - Some aspects of gravitational waves in an isotropic  
INT.REP.\* background Universe.
- IC/81/80 E. GAVA and R. JENGO - Perturbative evaluation of the thermal Wilson  
loop.
- IC/81/81 ABDUS SALAM and J. STRATHDEE - On the Olive-Montenon conjecture.  
INT.REP.\*
- IC/81/82 M.P. TOSI - Liquid alkali metals and alkali-based alloys as electron-  
INT.REP.\* ion plasmas.
- IC/81/83 M.A. EL-ASHRY - On the theory of parametric excitation of electron plasma.  
INT.REP.\*
- IC/81/84 P. BALLONE, G. SENATORE and M.P. TOSI - On the surface properties of a  
INT.REP.\* semi-infinite classical plasma model with permeable boundary.
- IC/81/85 G. CALUCCI, R. JENGO and M.T. VALLON - On the quantum field theory of  
charges and monopoles.
- IC/81/87 V.K. DOBREV, A.Ch. GANCHEV and O.I. YORDANOV - Conformal operators from  
spinor fields - I: Symmetric tensor case.
- IC/81/88 V.K. DOBREV - Stiefel-Skyrme-Higgs models, their classical static solutions  
and Yang-Mills-Higgs monopoles.
- IC/81/89 Trieste International Symposium on Core Level Excitations in Atoms,  
Molecules and Solids, 22-26 June 1981 (Extended abstracts).
- IC/81/90 A. TAWANSI, A.F. BASHA, M.M. MORSEI and S. EL-KONSOL - Effects of gamma-  
INT.REP.\* radiation and rare earth additives on the insulation of sodium silicate  
glasses.
- IC/81/91 A. TAWANSI, A.F. BASHA, M.M. MORSEI and S. EL-KONSOL - Investigation of  
INT.REP.\* the electrical conductivity of  $\gamma$ -irradiated sodium silicate glasses  
containing multivalence Cu ions.